Brain Research

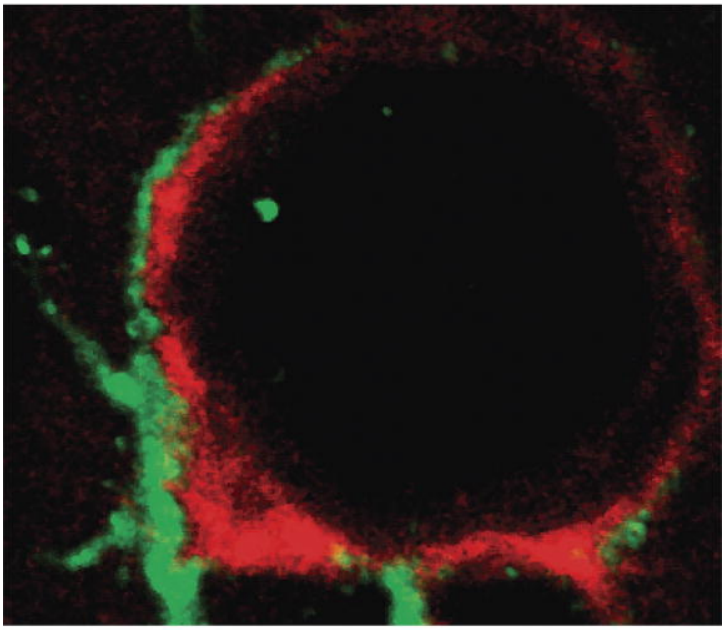

NOVEMBER 14, 2007 | VOLUME 1180
ISSN: 0006-8993

BRAIN RESEARCH 1180 (2007) 140–154

available at www.sciencedirect.com

ScienceDirect

www.elsevier.com/locate/brainres

BRAIN RESEARCH

Research Report

Evolution of the inflammatory response in the brain following intracerebral hemorrhage and effects of delayed minocycline treatment

Jason K. Wasserman[a,b], *Xiaoping Zhu*[a], *Lyanne C. Schlichter*[a,b,*]

[a]*Toronto Western Research Institute, University Health Network, Canada*
[b]*Department of Physiology, University of Toronto, Canada*

ARTICLE INFO

Article history:
Accepted 21 August 2007
Available online 5 September 2007

Keywords:
Stroke genes
Inflammatory cytokines, inflammatory proteins
Matrix metalloproteases
Tumor necrosis factor-α
Interleukin-1

ABSTRACT

There are no effective treatments for intracerebral hemorrhage (ICH). Although inflammation is a potential therapeutic target, there is a dearth of information about time-dependent and cell-specific changes in the expression of inflammation-related genes. Using the collagenase-induced ICH model in rats and real-time quantitative RT-PCR we monitored mRNA levels of markers of glial activation, pro- and anti-inflammatory cytokines, enzymes responsible for cytokine activation and several matrix metalloproteases at 6 h and 1, 3 and 7 days after ICH onset. For the most highly up-regulated genes, immunohistochemistry was then used to identify cell-specific protein expression. Finally, minocycline, a drug widely reported to reduce damage in several models of brain injury, was used to test the hypothesis that it can reduce up-regulation of inflammation-related genes when administered using a clinically relevant dosing regime: intraperitoneal injection beginning 6 h after ICH. Our results show a complex inflammatory response, with different brain cell types producing several pro- and anti-inflammatory molecules for at least 7 days after ICH onset. Included is the first demonstration that astrocytes are an important source of interleukin-1beta (IL-1β), interleukin-1 receptor antagonist (IL-1ra), interleukin-6 (IL-6) and MMP-12. Importantly, our results demonstrate that while delayed minocycline treatment effectively reduces early up-regulation of TNFα and MMP-12, its efficacy is lost when treatment is extended for up to a week, and it does not reduce several other genes associated with microglia activation. These results suggest caution in extrapolating to ICH the promising results of minocycline treatment in other models of brain injury.

1. Introduction

Intracerebral hemorrhage (ICH) is a devastating form of stroke, caused by rupture of a blood vessel in the brain. Every year, ICH affects about 120,000 people in the United States and represents 15–20% of all strokes (Wang and Dore, 2007). Mortality after ICH is higher than after ischemic stroke, and the prognosis for survivors is worse, but patient management is largely supportive and there are no effective drug treatments. During ICH, blood rapidly enters the brain parenchyma, disrupts delivery of oxygen and glucose to cells trapped inside the hematoma, and leads to neuron apoptosis and necrosis (Felberg et al., 2002; Qureshi et al., 2003; Wasserman and Schlichter, 2007). Early neurological deterioration (hours to

* *Corresponding author*. MC 9-417, 399 Bathurst Street, Toronto Ontario, Canada M5T 2S8. Fax: +1 416 603 5745.
E-mail address: schlicht@uhnres.utoronto.ca (L.C. Schlichter).

0006-8993/$ – see front matter © 2007 Elsevier B.V. All rights reserved.
doi:10.1016/j.brainres.2007.08.058

days) is associated with cerebral edema, brain swelling, increased intracranial pressure and hematoma enlargement. Extracellular matrix degradation and breakdown of the blood–brain barrier (BBB) by a family of proteolytic enzymes, the matrix metalloproteases (MMPs) (Rosenberg, 2002; Yong et al., 2001) contribute to disease severity.

In humans, deterioration and poor functional recovery correlate with a CNS inflammatory response that begins hours after ICH (Leira et al., 2004) and is characterized by activation of microglia and astrocytes, entry of peripheral immune cells and production of inflammatory mediators, including cytokines and MMPs (Wang and Dore, 2007). While inflammation is essential for wound healing, it is associated with BBB disruption and delayed neuron loss at the edge of the hematoma (Maier et al., 2006; Wasserman and Schlichter, 2007; Yenari et al., 2006). Diverse cytokines, produced primarily by glial cells, have been implicated in pro- and anti-inflammatory processes in response to brain injury (Barone and Feuerstein, 1999; Feuerstein et al., 1998; Lucas et al., 2006), and studies are beginning to characterize expression of inflammation-associated genes that might be involved in secondary brain injury after ICH. Two microarray studies (Lu et al., 2006; Tang et al., 2002) examined changes in gene expression, but only at 24 h after ICH. A major finding was that the early responses after ICH are substantially different from ischemia, hypoxia, hypoglycemia or seizures, with ~50% of the genes up-regulated in ICH being exclusive to this form of injury (Tang et al., 2002). Unfortunately, despite the large number of genes assessed in those two studies, very few inflammation-related genes were included.

In order to develop effective therapies for ICH, a better understanding is needed of the regulation and roles of genes that are changed during the progression of the injury. One compound, the tetracycline derivative, minocycline, which is being extensively tested in animal models of CNS injury, including spinal cord injury, ischemic stroke and hemorrhage, was initially thought to act simply by inhibiting microglial activation (Stirling et al., 2005; Yrjanheikki et al., 1998). However, it is now clear that minocycline acts through multiple processes, and since its efficacy can depend on the injury type and severity and can even be adverse (Tsuji et al., 2004), its actions must be further examined. Some recent experimental ICH studies have tested minocycline, and important differences in experimental design and outcome measures can provide valuable insights (see Discussion). One study (Power et al., 2003) measured expression of MMPs in remote tissue as much as 4 mm from the hematoma and reported that minocycline treatment, begun 1 h after ICH onset, reduced MMP-12 expression at 7 days and improved functional recovery. We found that neurons did not die in this remote region, but neuron death continued in the tissue immediately adjacent to the hematoma for up to 3 days (Wasserman and Schlichter, in press). When we delayed minocycline treatment for 6 h after ICH onset, it did not prevent this neuron death, but it reduced BBB breakdown, edema and the early expression of TNFα and MMP-12 (Wasserman and Schlichter, in press; Wasserman and Schlichter, 2007). Another study (Szymanska et al., 2006) used much larger ICH lesions and addressed the effect of minocycline (begun at 3 h) on neuron survival and functional recovery. No functional improvement was seen although it is possible that the large hematoma volume might have limited the potential for recovery. An appreciation of the importance of inflammation, BBB breakdown and edema after ICH has now prompted us to examine in more detail the effect of delayed minocycline treatment. Thus, the purpose of the present study was to monitor changes in both the acute (6 h) and delayed (1, 3, 7 days) expression of numerous genes related to inflammation and BBB breakdown, to determine which cells produce the major molecules as the inflammatory response evolves and to assess the effects of delayed minocycline treatment on these mediators.

2. Results

2.1. *Changes in microglia and astrocyte activation markers after ICH*

Reactive gliosis following brain injury involves activation of microglia and astrocytes, which is characterized by up-regulation of complement receptor 3 (CR3) and glial fibrillary acidic protein (GFAP), respectively (Pekny and Nilsson, 2005; Streit et al., 1999). Not surprisingly, in the ipsilateral striatum, real-time quantitative RT-PCR showed a short lag time and then consistent up-regulation of CR3 and GFAP mRNA expression (Fig. 1). That is, at 1, 3 and 7 days after ICH, CR3 increased by 2.3, 6.6 and 5.8 fold, and GFAP increased by 3.0, 3.6 and 3.3 fold, compared with sham-operated controls. On the contralateral side of the brain, neither gene changed significantly.

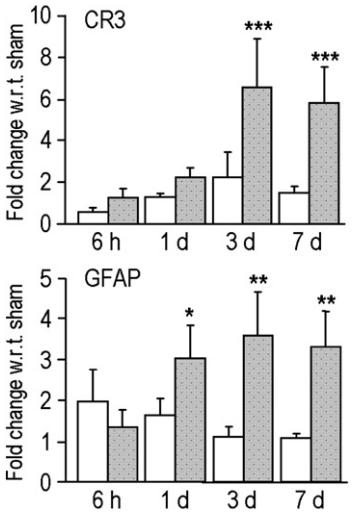

Fig. 1 – Changes in mRNA expression of microglia and astrocyte cell markers after ICH. Complement receptor 3 (CR3) and glial fibrillary acid protein (GFAP) were used as markers of microglia/macrophages and astrocytes, respectively. Gene expression was monitored by real-time qRT-PCR in the contralateral (white bars) and ipsilateral striatum (gray bars) from 6 h to 7 days after ICH onset. The *y*-axis shows relative gene expression (fold changes); normalized to time-matched sham-operated animals (see Experimental procedures for details). Significant differences are indicated as: $^{*}p<0.05$, $^{**}p<0.01$, $^{***}p<0.005$ (ANOVA, followed by Bonferroni correction; 4–5 rats for each time point).

2.2. *Time-dependent increases in expression of specific cytokine genes and converting enzymes*

We monitored mRNA expression of several genes using real-time RT-PCR (Fig. 2), from shortly after ICH onset (6 h) until the wound was considerably resolved (7 days; see Fig. 9). These genes included the pro-inflammatory genes, tumor necrosis factor alpha (TNFα) and the interleukins, -1beta (IL-1β) and -6 (IL-6); the generally anti-inflammatory genes, interleukin-10 (IL-10), transforming growth factor beta (TGFβ); and the endogenous interleukin-1 receptor antagonist (IL-1ra). Because the mature forms of TNFα and IL-1β are produced by cleavage of

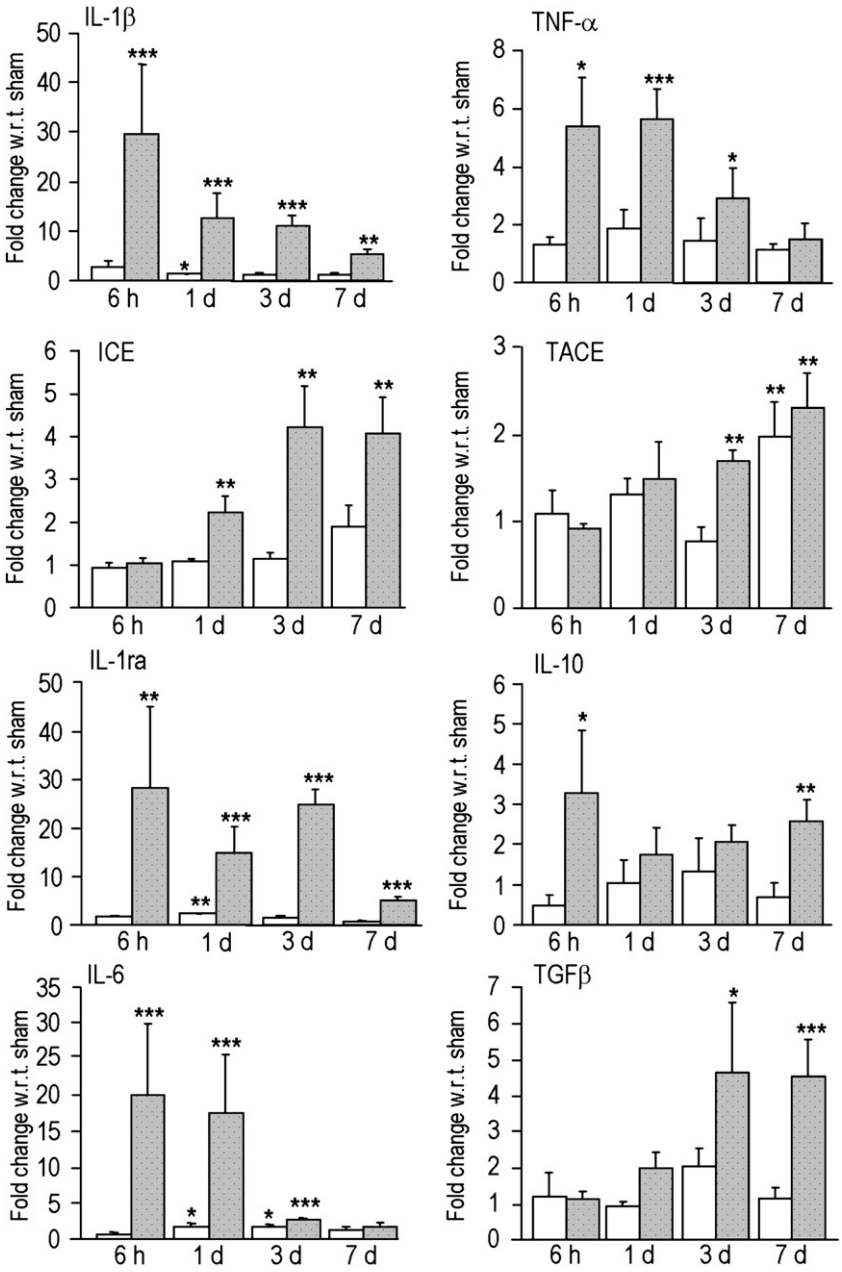

Fig. 2 – Temporal pattern of expression of cytokine-related genes. Changes in mRNA expression were monitored by quantitative real-time RT-PCR for several genes related to cytokine regulation. Comparisons were between animals subjected to ICH and sham-operated animals, with expression assessed in both the contralateral (white bars) and ipsilateral striatum (gray bars) from 6 h to 7 days after ICH onset. All values on the y-axes are expressed as fold changes, normalized to time-matched sham-operated control animals (see Experimental procedures). Note the similar time profile of up-regulation of the three pro-inflammatory cytokines, TNFα, IL-1β and IL-6, and delayed increases in TNFα converting enzyme (TACE), which processes TNFα, and IL-1 converting enzyme (ICE), which processes IL-1β. Three anti-inflammatory genes, IL-10, TGFβ and IL-1ra, were also up-regulated. Significant differences are indicated as: *$p<0.05$, **$p<0.01$, ***$p<0.005$ (ANOVA, followed by Bonferroni correction; 4–5 rats for each time point).

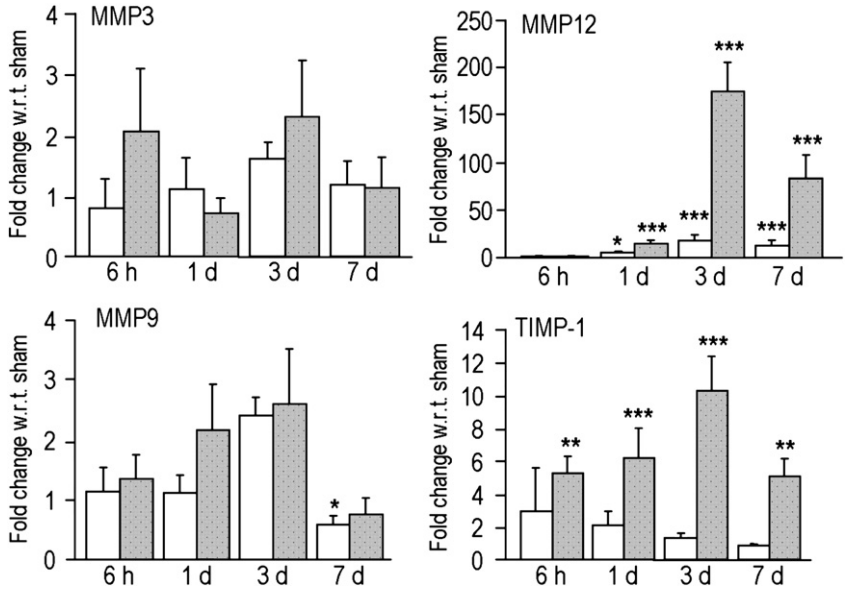

Fig. 3 – Temporal changes in the expression of matrix metalloprotease-related genes. mRNA expression was compared in the contralateral (white bars) and ipsilateral (gray bars) striatum, using qRT-PCR from 6 h to 7 days after ICH onset. Values on the y-axes are expressed as fold changes, normalized to time-matched sham-operated control animals. Note the very large increases in MMP-12 expression. Significant differences are indicated as: *$p<0.05$, **$p<0.01$, ***$p<0.005$ (ANOVA, followed by Bonferroni correction; 4–5 rats for each time point).

their precursor molecules, we also quantified changes in their converting enzymes, TNFα converting enzyme (TACE) and IL-1 converting enzyme (ICE). *IL-1β.* IL-1β expression in the ipsilateral striatum increased rapidly and dramatically and then resolved considerably by 7 days. At 6 h and 1, 3 and 7 days the increases were 29.7, 12.6, 10.9 and 5.3 fold. There was also a very slight response on the contralateral side; e.g., a 1.4 fold increase at 1 day. *ICE.* The interleukin-1 converting enzyme increased later than IL-1β and then remained elevated until the end of the 7 day test period. The change was moderate: 2.2, 4.2 and 4.0 fold at 1, 3 and 7 days in the ipsilateral striatum. *IL-1ra.* IL-1ra, the endogenous inhibitor of IL-1β, was rapidly and dramatically up-regulated and remained elevated for a few days; much like the changes in IL-1β itself. Increases in the ipsilateral side were 28.0, 14.8, 24.9 and 5.0 fold at 6 h, 1, 3 and 7 days. *IL-6.* IL-6 expression in the ipsilateral striatum also increased rapidly and considerably and then resolved between 3 and 7 days. The increases were 20.0, 17.5, 2.6 and 1.7 fold at 6 h, 1, 3 and 7 days. There was a small but significant response on the contralateral side: 1.8 fold and 1.6 fold at 1 and 3 days. *TNFα.* In the ipsilateral striatum, TNFα expression increased immediately, but to a much lower degree than IL-1β and IL-6, and then it resolved between 1 and 7 days. Specifically, at 6 h, 1 day and 3 days, the mRNA levels increased by 5.3, 5.4, and 2.9 fold compared with time-matched sham-operated animals. *TACE.* Expression of the TNFα converting enzyme increased after a delay; i.e., with a similar time course to ICE but a smaller change. In the ipsilateral striatum it increased 1.7 fold at 3 days and 2.3 fold at 7 days. TACE also increased slightly on the contralateral side: by 2 fold at 7 days. *IL-10.* Interestingly, expression of the anti-inflammatory cytokine IL-10 increased significantly in a biphasic manner. The increases were 3.3 and 2.6 fold at 6 h and 7 days. *TGFβ.* Up-regulation of TGFβ was delayed compared with the other cytokines and displayed a similar time course to CR3 and GFAP (compare with Fig. 1). It increased modestly in the ipsilateral striatum: 4.6 and 4.5 fold at 3 and 7 days.

2.3. *Temporal changes in expression of matrix metalloprotease-related genes*

Expression of several matrix metalloproteases (MMP-3, MMP-9 and MMP-12) and the endogenous tissue inhibitor of the metalloproteinases (TIMP-1) was monitored from 6 h to 7 days after ICH onset (Fig. 3). MMP-3 and MMP-9 expression did not change between 6 h and 7 days after ICH onset. Interestingly, at 7 days, MMP-9 expression on the contralateral side of ICH animals was lower than in control animals. *MMP-12.* This was the most highly up-regulated of all 14 genes examined. The increase was significant by day 1 (by 13.9 fold), peaking at 3 days (174.9 fold) and beginning to resolve by 7 days (83.8 fold). There was a similar time course but much less up-regulation on the contralateral side: 4.3, 17.8 and 12.2 fold at 1, 3 and 7 days. *TIMP-1.* The endogenous inhibitor was rapidly up-regulated and, like MMP-12, it peaked at 3 days and began to resolve by 7 days. Increases in the ipsilateral side were 5.2, 6.2 and 10.3 and 5.1 fold at 6 h and 1, 3 and 7 days. Of note, the TIMP-1 rise at 6 h preceded increases in the MMPs.

2.4. *Effects of delayed minocycline treatment on gene expression*

The temporal expression profile of the same 14 genes was monitored when minocycline treatment was begun 6 h after ICH onset and continued for either 3 or 7 days. Results were compared with time-matched vehicle-treated animals. Fig. 4 shows only the 5 genes whose expression was significantly

affected. There were a few indications of a reduced inflammatory response but the minocycline-dependent changes were generally small and short-lived. For instance, on the ipsilateral side, the ICH-induced up-regulation of TNFα expression was reduced by minocycline at 1 day: from a 5.6 to a 3.7 fold increase. IL-1β was reduced on day 7, but only when minocycline treatment lasted the full 7 days. The interleukin-1 converting enzyme, ICE, declined from a 2.2 to a 1.7 fold increase at 1 day, but it rebounded by day 3 and showed an increasing trend at day 7. Furthermore, minocycline reduced expression of the anti-inflammatory IL-1 receptor antagonist (IL-1ra) at 3 days: from 24.6 fold to 17.5 fold. Minocycline transiently reduced the ICH-induced up-regulation of MMP-12, first on the contralateral and then on the ipsilateral side; e.g., from a 174.9 to a 96.8 fold increase at 3 days. However, the normal spontaneous MMP-12 decline between days 3 and 7 (from 174.9 to 83.8 fold in vehicle-treated animals) was partly reversed by minocycline treatment: to 139.2 fold.

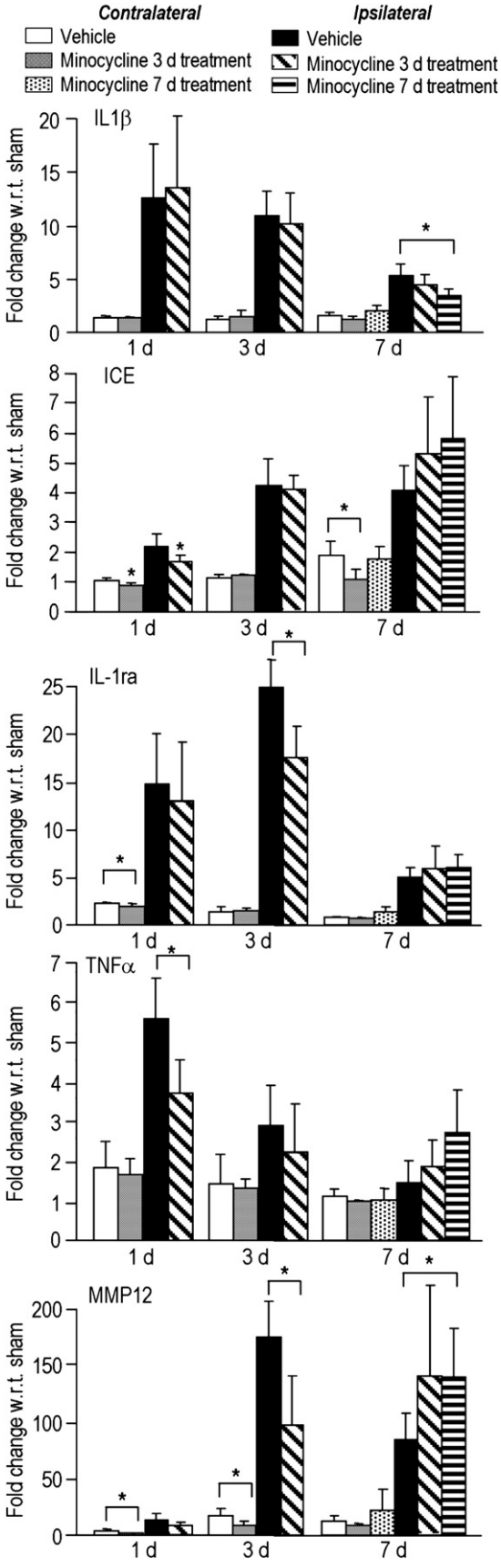

Fig. 4 – Effects of delayed minocycline treatment on gene expression. Gene expression was monitored in animals treated with minocycline and compared with control animals injected with an equal amount of saline. Within the treatment group, minocycline was administered for either 3 days or 7 days. Animals were sacrificed at 1, 3 or 7 days after ICH onset. The *x*-axes indicate when the animals were sacrificed. Values on the *y*-axes are expressed as fold changes, normalized to time-matched sham-operated animals. Significant differences between vehicle and minocycline treatment groups are indicated as: *$p<0.05$ (ANOVA, followed by Bonferroni correction; $n=4$–5 rats for each treatment group).

2.5. *Cellular and temporal expression of selected proteins after ICH*

Based on the very large increases in mRNA expression of IL-1β, IL-1ra, IL-6 and MMP-12, we performed immunohistochemistry to examine the temporal expression and cellular sources of these four proteins. Frozen brain sections were prepared from animals sacrificed at 6 h and 1, 3 or 7 days after ICH. An antibody against GFAP was used to visualize astrocytes, and tomato lectin was used to visualize microglia/macrophages and endothelial cells. Activated microglia were identified as small lectin-positive cells with short, irregular processes. Lectin-positive endothelial cells surrounded blood vessels, ranging in size from large circular arterioles to small narrow capillaries.

The interleukin-related molecules showed clear time- and cell-specific distributions after ICH. *IL-1β* (Fig. 5). Both the prevalence and cell types stained changed with time. In the ipsilateral striatum, IL-1β staining at early times (6 h, 1 day) was observed predominantly in amoeboid or spherical ('activated') microglia/macrophages and almost exclusively at the edge of the hematoma. At later times (3 and 7 days), very few IL-1β positive microglia/macrophages were observed; however, IL-1β positive astrocytes were seen throughout the intact part of the striatum surrounding the hematoma. Interestingly, in the contralateral striatum, there were a few IL-1β positive astrocytes at 1 day after ICH. *IL-1ra* (Fig. 6). Immunoreactivity was largely restricted to astrocytes in the ipsilateral striatum, and the staining appeared to increase with time as the number of

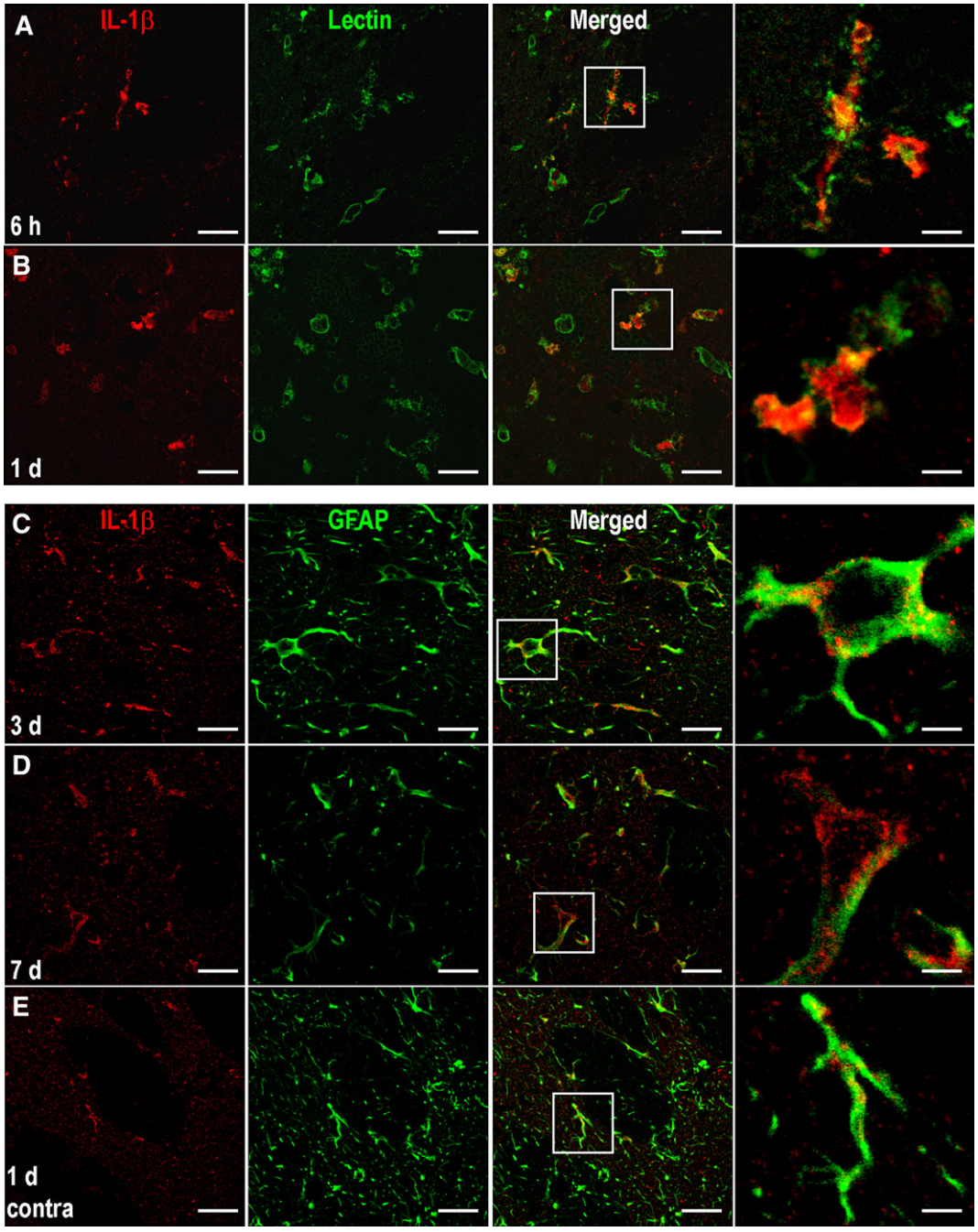

Fig. 5 – Cellular expression of IL-1β immunoreactivity in the striatum after ICH. Representative confocal micrographs from the striatum 6 h to 7 days after ICH onset, labeled with IL-1β (red), and GFAP (astrocytes, green) or tomato lectin (endothelial cells and microglia, green). Areas within the white boxes are shown at higher magnification to the right. (A, B) At 6 h and 1 day after ICH, IL-1β was detected primarily in tomato lectin-positive activated microglia/macrophages at the edge of the hematoma. It did not co-localize with tomato lectin-positive endothelial cells surrounding blood vessels. (C, D) At 3 and 7 days after ICH, IL-1β was detected in GFAP positive astrocytes in the ipsilateral striatum. (E) In the contralateral striatum, IL-1β was also detected in GFAP positive astrocytes at 1 day after ICH. Scale bar, 25 μm (5 μm in magnified images).

reactive astrocytes surrounding the hematoma increased. In some animals, there were a small number of thin, IL-1ra positive processes (possibly from microglia), but IL-1ra was not detected in microglia cell bodies (not shown). In the contralateral striatum, a few astrocytes became immunoreactive for IL-1ra at 3 days. *IL-6* (Fig. 7). IL-6 had a similar astrocytic distribution to IL-1ra. From 6 h to 7 days after ICH, it was mainly in astrocytes surrounding the hematoma, and its apparent increase with time paralleled the increase in GFAP staining. IL-6 did not co-localize with tomato lectin-positive microglia/macrophages (not shown). Particularly interesting was the IL-6 staining at 1 day in some blood vessels surrounding the hematoma, typically in moderate caliber vessels that were likely arterioles. Although IL-6 co-localized with tomato lectin-positive endothelial cells, it was

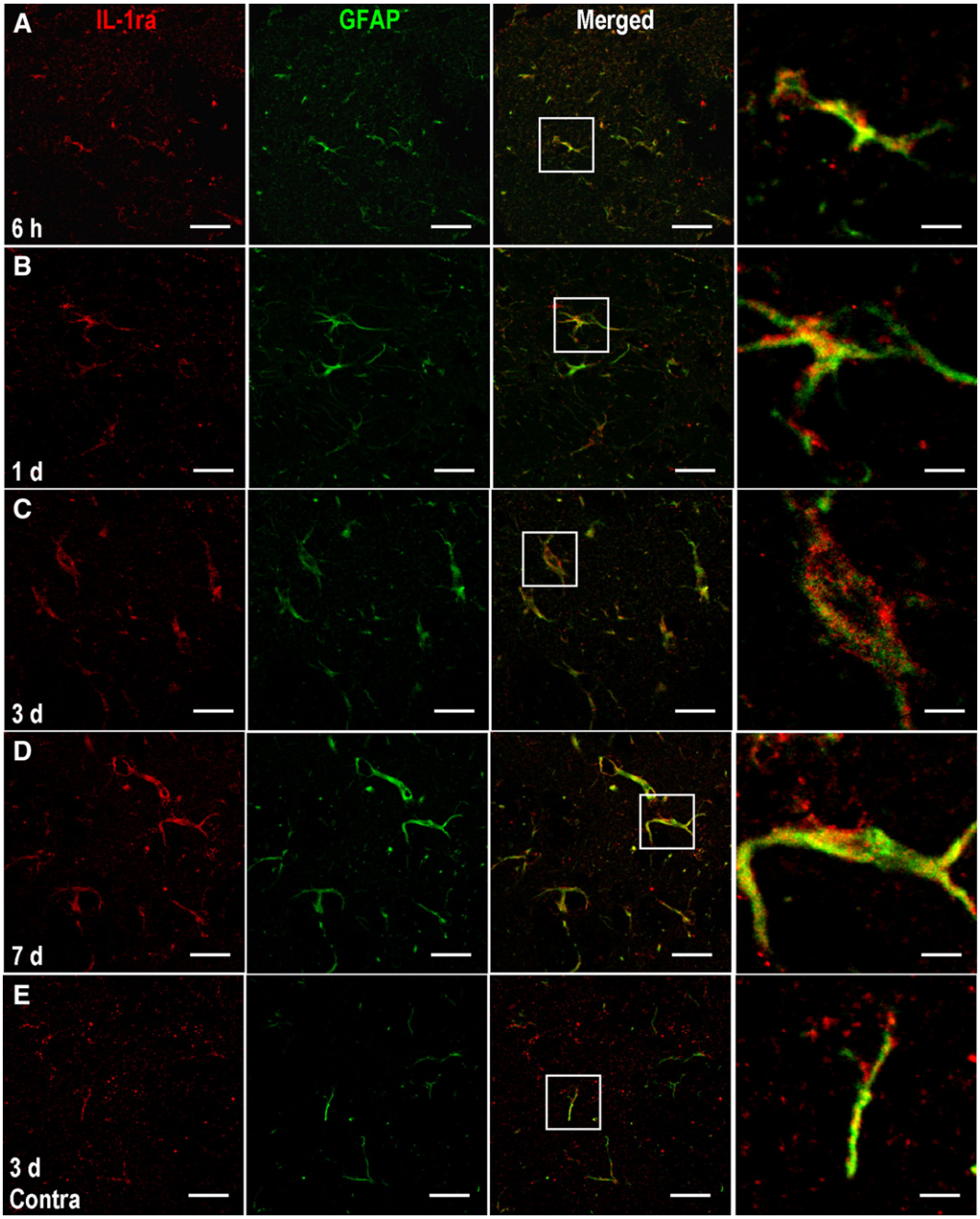

Fig. 6 – IL-1ra immunoreactivity in the striatum after ICH. Representative confocal micrographs show immunolocalization of IL-1β (red) and GFAP (astrocytes, green). Areas within the white boxes are shown at higher magnification to the right. (A–D) The ipsilateral striatum is shown from 6 h to 7 days after ICH onset. IL-1ra staining was detected primarily in GFAP positive astrocytes. (E) In the contralateral striatum, IL-1ra was also detected in GFAP positive astrocytes at 3 days after ICH onset. Scale bar, 25 μm (5 μm in magnified images).

predominantly on the luminal side of the vessel. IL-6 staining was also observed in some blood vessels in the contralateral striatum after ICH (not shown).

MMP-12 (Fig. 8). Both the prevalence and cell types showing MMP-12 immunoreactivity changed with time after ICH. Whereas MMP-12 was not detected in astrocytes at 1 day, they became the main source at 3 days (Figs. 8A, B), and a small number remained positive at 7 days (not shown). Pronounced MMP-12 staining was present from 1 to 7 days in the extracellular space between astrocytes and endothelial cells; i.e., in the basal lamina surrounding blood vessels (Figs. 8D–F). This staining was restricted to moderately sized vessels (~50 μm diameter), with a minority of them (<25%) labeled in the striatum surrounding the hematoma. In addition, MMP-12 staining was occasionally observed throughout the somata and proximal processes of large (>25 μm diameter) GFAP-negative cells (e.g., Fig. 8A). Their size and morphology are only consistent with neurons within the striatum, and they

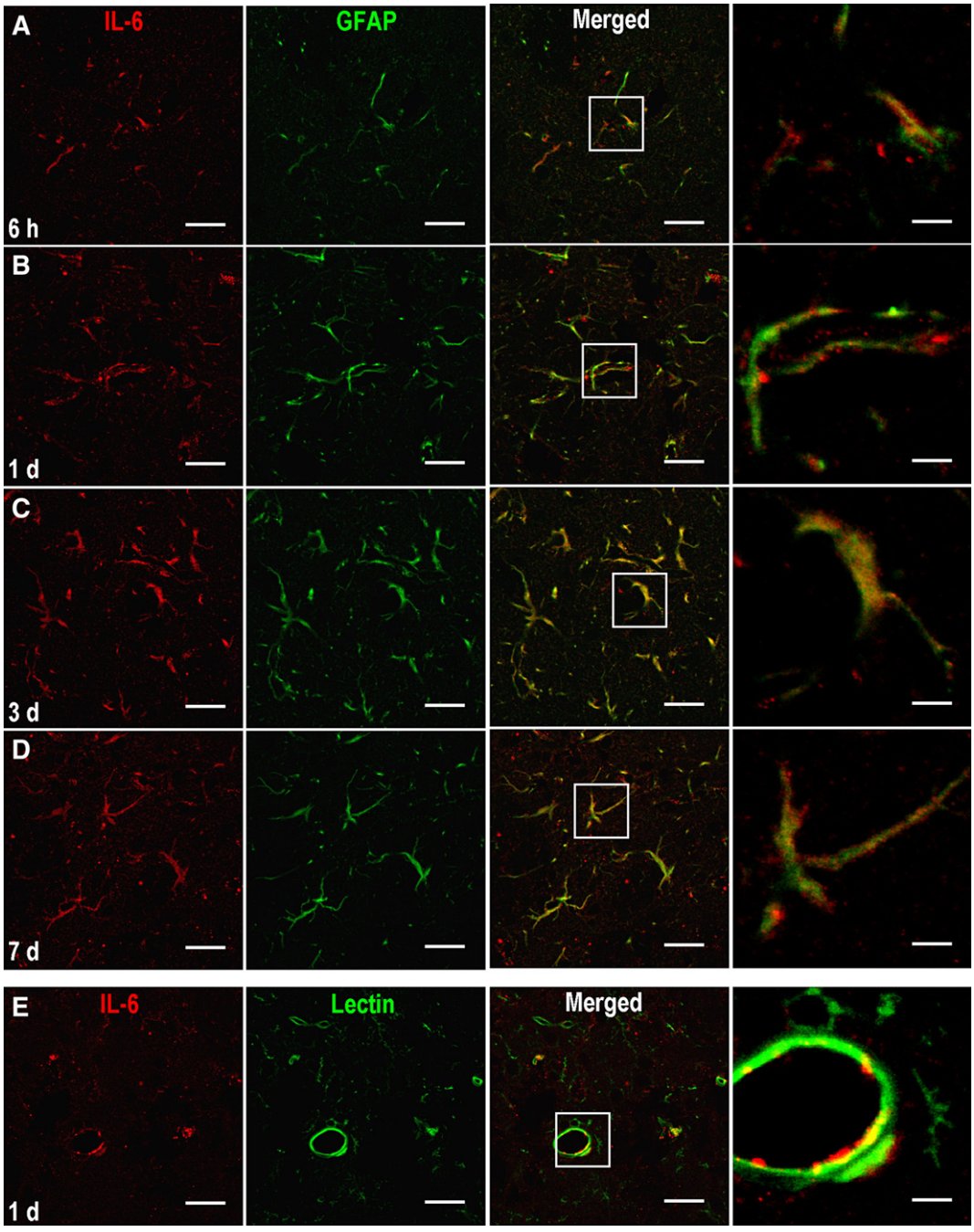

Fig. 7 – IL-6 immunolocalization in the striatum after ICH. Representative confocal micrographs from the ipsilateral striatum, showing immunoreactivity for IL-6 (red) and GFAP (astrocytes, green) or tomato lectin (endothelial cells and microglia/macrophages, green). Areas within the white boxes are shown at higher magnification to the right. (A–D) From 6 h to 7 days after ICH onset, IL-6 staining was detected primarily in GFAP positive astrocytes. (E) IL-6 was observed inside and adjacent to tomato lectin-positive endothelial cells surrounding blood vessels, but not within lectin-positive microglia/macrophages. Scale bar, 25 μm (5 μm in magnified images).

label with the neuronal marker, microtubule associated protein-2 (Wasserman and Schlichter, in press). In contrast with MMP-12 immunoreactivity in astrocytes, neurons and basal lamina, MMP-12 was co-localized with only a small number of activated microglia/macrophages in the injured striatum. However, MMP-12 was present in the extracellular space surrounding microglia/macrophages in the hematoma and adjacent striatum (not shown).

3. Discussion

This report includes the most comprehensive study of gene expression during the evolving inflammatory response after experimental ICH. Genes were selected to focus on pro- and anti-inflammatory mediators and on matrix metalloproteases (MMPs), which have been implicated in BBB breakdown and

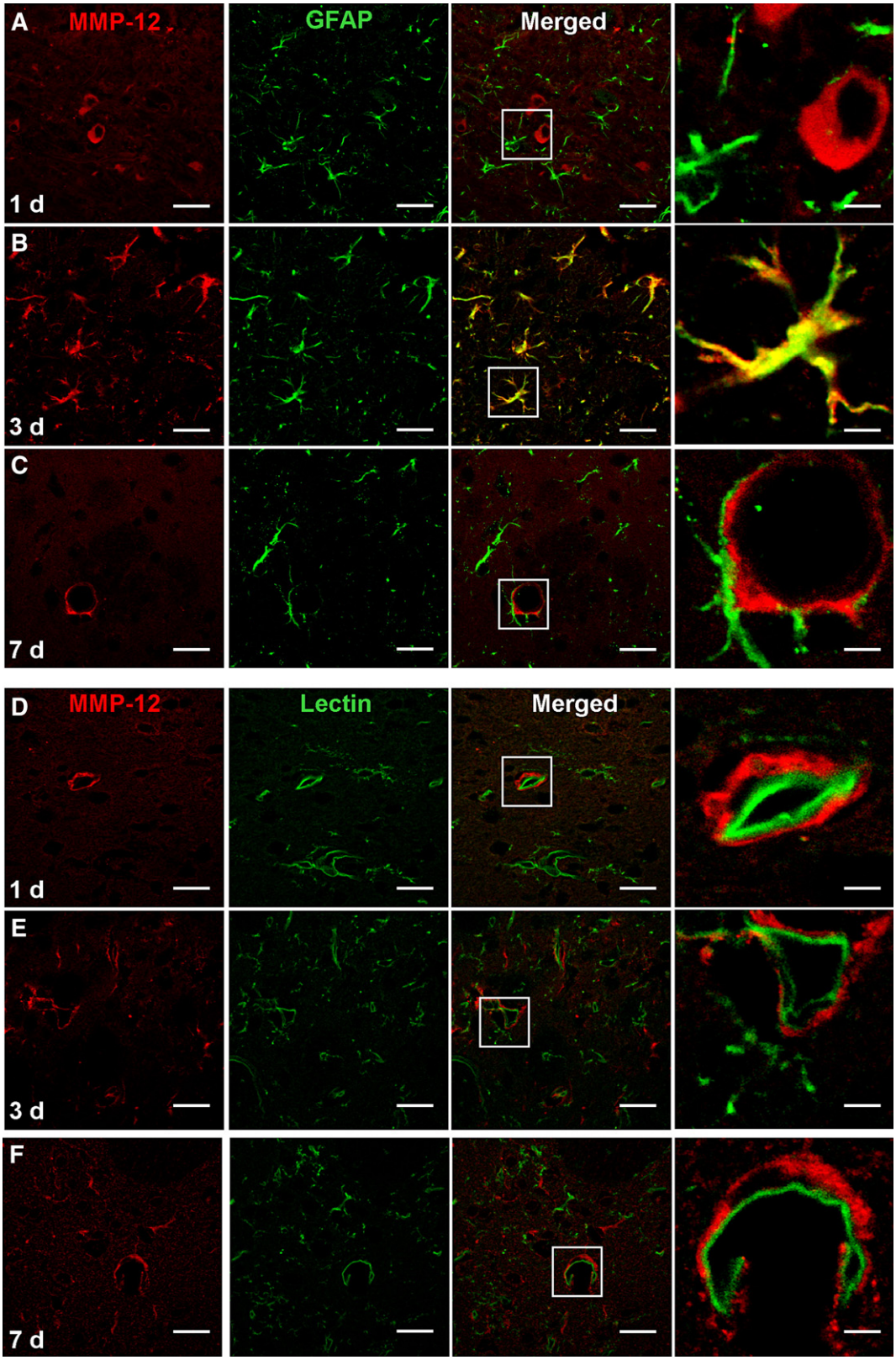

Fig. 8 – MMP-12 immunolocalization in the striatum after ICH. Representative confocal micrographs from the ipsilateral striatum, showing immunoreactivity for MMP-12 (red) and GFAP (astrocytes, green) or tomato lectin (endothelial cells and microglia/macrophages, green). Areas within the white boxes are shown at higher magnification to the right. (A) At 1 day after ICH onset, MMP-12 was detected primarily in large cells that did not label for GFAP. (B) At 3 days, MMP-12 was abundant in GFAP positive astrocytes. (C–F) MMP-12 staining was pronounced around blood vessels but did not co-localize with tomato lectin-positive endothelial cells. Instead, staining was adjacent to GFAP positive astrocytes (C) and endothelial cells (D–F) from 1 to 7 days after ICH onset. Scale bar, 25 μm (5 μm in magnified images).

edema, parameters that are important in determining the outcome of ICH. Fourteen genes were monitored simultaneously by quantitative real-time RT-PCR (qRT-PCR), and several important time points were chosen; i.e., from the time of maximal hematoma development (6 h) until the wound was largely resolved (7 days). Importantly, to distinguish between ICH-specific changes and surgery-induced responses, expression of every gene was normalized to sham-operated animals that were time-matched. Then, to assess minocycline-dependent changes in gene expression, we delivered the drug at a clinically relevant time using intraperitoneal injection beginning 6 h after ICH onset. Immunohistochemistry was then used to determine the cellular sources of the most highly up-regulated genes at the same time points used for qRT-PCR analysis. There are several key findings. *(i)* The injured striatum produces both pro- and anti-inflammatory mediators for at least 7 days after ICH onset. *(ii)* Transcript expression of the pro-inflammatory cytokines rises rapidly (by 6 h after ICH onset) and then begins to resolve while their converting enzymes are up-regulated. Thus, the striatum apparently counteracts pro- with anti-inflammatory responses as early as 6 h after ICH onset. *(iii)* The cellular sources of IL-1β, IL-6, IL-1ra and MMP-12 proteins change during the 7 day time course. At later times, from 3 to 7 days after ICH onset, astrocytes become an important source of IL-1β, IL-6, IL-1ra and MMP-12. *(iv)* Delayed minocycline treatment reduces the ICH-induced up-regulation of TNFα and MMP-12; however, it is apparently a more effective inhibitor of microglial activation after ischemic stroke (Yrjanheikki et al., 1998, 1999).

Limited data are available regarding the relationship between pro- and anti-inflammatory cytokines in the hours and days after ICH onset, despite cytokines having been implicated in the pathogenesis of ICH. It is particularly important to study TNFα and IL-1β, which have been described as 'orchestrators' of the inflammatory response, that activate the endothelium and promote entry of peripheral leukocytes (Barone and Feuerstein, 1999). In doing so, they can worsen the outcome; e.g., after experimental ischemic stroke, brain injury was increased by injecting IL-1β into the striatum (Stroemer and Rothwell, 1998). We found that IL-1β mRNA was nearly absent from the healthy striatum but was dramatically up-regulated within 6 h after ICH. Its damage-specific up-regulation makes it an attractive therapeutic target, provided that IL-1β-reducing strategies can be applied soon enough after ICH onset. Although TNFα was up-regulated in the same rapid time frame (but to a lesser degree than IL-1β), the protein was expressed in the healthy striatum and is required for normal brain function (Bruce et al., 1996). Hence, if a treatment ablates TNFα, it might produce unacceptable side effects. An alternative approach to inhibiting these cytokines is to reduce their converting enzymes (ICE, TACE), which are required to produce the mature cytokines (Black et al., 1997; Moss et al., 1997; Wilson et al., 1994). IL-1β and TNF-α mRNA decreased as ICE and TACE mRNA levels underwent a later increase (at 3 and 7 days). This inverse relationship likely reflects a lag between mRNA and protein expression. A limitation of this study is that it did not measure ICE and TACE protein levels and, more importantly, the activity of these enzymes.

Another approach to re-balance the inflammatory response is to increase expression of endogenous anti-inflammatory factors such as IL-1ra, IL-10 and TGFβ. In previous animal studies of ischemic stroke, artificially increasing IL-1ra was effective and the lesion was decreased by injecting IL-1ra into the brain or by over-expressing the IL-1ra gene (Loddick and Rothwell, 1996; Mulcahy et al., 2003; Yang et al., 1997). A similar strategy might prove effective for ICH since time-dependent increases in IL-1β expression were paralleled by increases in its endogenous antagonist, IL-1ra (present study), and over-expressing IL-1ra reduced edema in a rat model of ICH (Masada et al., 2001). Interestingly, we found that the cellular sources of IL-1β and IL-1ra changed with time after ICH. Activated microglia/macrophages were the major source of IL-1β protein at early times, supporting their role in initiating the early inflammatory response. At later times, astrocytes contained IL-1β, raising the possibility that they sustain the inflammation. However, astrocytes were also the major source of IL-1ra at all times examined, which suggests a simultaneous balancing of pro- and anti-inflammatory phenotypes. Their delayed IL-1β production might also act in an autocrine fashion to stimulate production of neurotrophic factors that support tissue repair and regeneration (Liberto et al., 2004).

The present study shows that IL-6 mRNA expression was highly up-regulated within 6 h and remained elevated for at least 24 h, with astrocytes and endothelial cells containing IL-6 protein for at least 7 days after ICH onset. Human cerebral endothelial cells can produce IL-6 (Kallmann et al., 2002). Our observation of IL-6 protein in endothelial cells of large blood vessels around the hematoma suggests that they release it into the blood after ICH, and if so, IL-6 in the plasma of ICH patients may be brain derived. Although IL-6 is traditionally categorized as a pro-inflammatory cytokine, contradictory effects have been reported after brain injury. IL-6 knockout mice had similar infarct volumes and neurological impairment 24 h after focal ischemia (Clark et al., 2000), but this result is difficult to interpret because their TNFα, IL-1β and IL-1ra mRNA levels were also ~50% lower than in wild-type mice. In humans, high plasma IL-6 levels correlated with poor neurological outcome after ischemic or hemorrhagic stroke (Leira et al., 2004; Vila et al., 2000), but it is unclear whether increased IL-6 was a cause or result of worse damage. In animal studies, IL-6 promoted astrogliosis, and its over-expression by astrocytes disrupted the blood–brain barrier during development (Brett et al., 1995). Conversely, IL-6 promoted wound healing after experimental focal brain injury (Penkowa et al., 2003), and injecting it into the brain after focal ischemia decreased the injury volume (Loddick et al., 1998). Moreover, after traumatic brain injury in humans, elevated levels of IL-6 in the cerebral spinal fluid correlated with an improved outcome (Singhal et al., 2002).

Matrix metalloproteases (MMPs) are thought to exacerbate brain injury following ICH (Rosenberg, 2002; Yong et al., 2001). Most animal ICH studies have focused on MMP-9 (Lee et al., 2005; Wang and Tsirka, 2005; Xue and Del Bigio, 2000; Zhao et al., 2006), probably based on human studies correlating MMP-9 protein levels in the brain and blood with the severity of brain injury (Abilleira et al., 2003; Alvarez-Sabin et al., 2004; Rosell et al., 2006; Silva et al., 2005). Although MMP-9 was found in astrocytes after experimental ICH (Tejima et al., 2007), MMP-12 appears to be the most highly up-regulated MMP in the brain after ICH (Power et al., 2003). Power et al. (2003) sampled remote tissue (2–4 mm from the hematoma) and showed a substantial

delay (7 days) before MMP-12 mRNA dramatically increased, and the protein was present in the extracellular space around apparently activated microglia/macrophages. Here, by sampling tissue in the peri-hematoma region very close to the bleed and in the adjacent striatum, we found earlier dramatic increases in MMP-12 mRNA; i.e., from 1 to 7 days after ICH onset, and found that astrocytes are a major source of MMP-12 protein after ICH. Like Power et al. (2003), we observed MMP-12 immunoreactivity in the extracellular space around amoeboid and spherical (activated) microglia/macrophages. Endothelial cells can produce MMP-12 *in vitro* (Hummel et al., 2001), and we also observed staining adjacent to, but not inside these cells from 1 to 7 days after ICH. A lack of cytoplasmic MMP-12 staining likely reflects a high rate of protein release. MMP-12 staining in endothelial cells is consistent with and extends our previous observation that this enzyme is present in the basal lamina of damaged blood vessels at 1 and 3 days after ICH (Wasserman and Schlichter, in press). Because MMP-12 can degrade various components of the basal lamina, including the major constituent type IV collagen (Chandler et al., 1996), it may contribute to acute blood–brain barrier damage and delayed vascular remodeling.

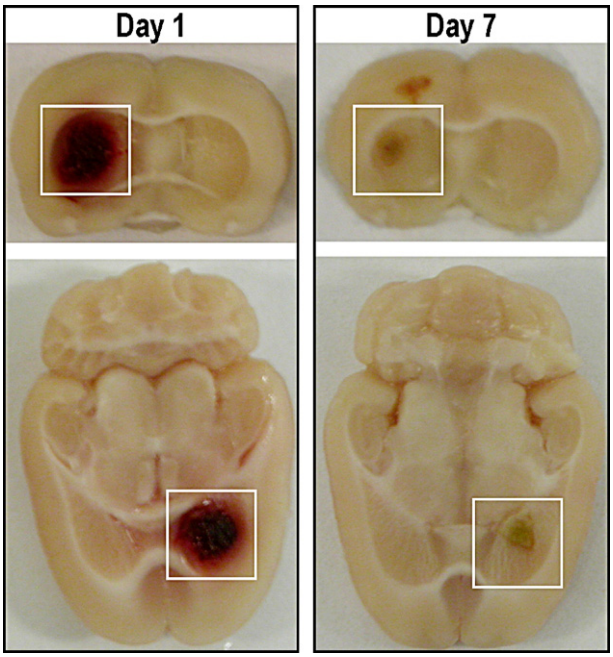

Fig. 9 – The model of intracerebral hemorrhage (ICH) in the rat striatum. Representative brains, dissected at 1 and 7 days after ICH onset, were sliced coronally (upper panel) through the middle of the hematoma (at bregma; showing the dorsal–ventral axis) or in the horizontal plane (lower panel) through the middle of the hematoma (~5 mm ventral to bregma; showing the rostral–caudal axis). The hematoma was located primarily in the anterior portion of the striatum, particularly in the caudate, and occupied a large area at Day 1, but was much smaller at Day 7, owing to wound resolution and tissue atrophy. In most animals, the volume of the hematoma at Day 1 was similar to the volume at 6 h. The white boxes illustrate typical areas of tissue sampled for quantitative real-time reverse-transcriptase polymerase chain reaction (qRT-PCR).

In comparing effects of treatment with minocycline following ICH, it is important to consider differences in experimental design. ICH causes neutrophil infiltration, microglial activation and migration to the injured site, processes that are inhibited by minocycline (Power et al., 2003; Wasserman and Schlichter, 2007). However, it is important to investigate other potential targets of minocycline action. Inflammatory genes (e.g., CR3, TNFα, IL-1β) are also up-regulated after ICH, and although we detected microglia activation and found that they were the major early source of IL-1β, minocycline treatment was ineffective in reducing either CR3 or IL-1β (not shown). We previously found that minocycline reduced infiltration of neutrophils (Wasserman and Schlichter, in press), and since they were the major source of TNFα after ICH, the minocycline-dependent decrease in TNFα expression at 1 day is likely due to fewer neutrophils rather than effects on microglia. MMP-12 has been implicated in the damage after ICH since sensorimotor recovery was improved in MMP-12 knockout mice (Wells et al., 2005), and minocycline treatment reduced MMP-12 gene expression, blood–brain barrier damage, edema (Wasserman and Schlichter, in press) and neurological deficits (Power et al., 2003). Taken together, the published results support a substantial role for MMP-12 in the pathogenesis of ICH, and the specific effects help explain why minocycline improves functional outcome without apparently reducing neuron death after ICH. An important conclusion from this work is that MMP-12 expression should be assessed in human ICH patients where similar findings would support a therapeutic strategy to selectively target this enzyme. Moreover, since MMP-12 is not expressed in the healthy brain, targeting this enzyme should have fewer side effects than using broad-spectrum MMP inhibitors or targeting MMP-9, which is expressed in the healthy brain (Zhao et al., 2006). A cautionary note is that, in the present study, delayed minocycline treatment reduced MMP-12 expression in the striatum on day 3 but, surprisingly, MMP-12 rebounded at day 7 when minocycline treatment was continued for 7 days. Although effects of minocycline might depend on the route and timing of administration or on whether MMP-12 expression is measured near or far from the hematoma, it remains possible that minocycline is protective through actions other than reducing MMP-12.

4. Experimental procedures

4.1. *Animals, surgeries and induction of intracerebral hemorrhage*

Male Sprague–Dawley rats (300–350 g; Charles River) were maintained under a 12 h light/dark cycle, with food and water available *ad libitum*. All procedures were approved by the University Health Network animal care committee, in accordance with guidelines established by the Canadian Council on Animal Care. Intracerebral hemorrhage was induced in the striatum (Fig. 9) using a method developed by Rosenberg et al. (1990) with several previously described modifications (Wasserman and Schlichter, 2007). In brief, rats were anesthetized using isofluorane (3% induction, 1.5% maintenance) and placed in a stereotaxic frame. Under aseptic conditions, a 1 mm diameter burr hole was drilled in the skull (0.2 mm anterior and 3 mm

lateral to bregma) and a 30-gauge needle was lowered into the right caudate putamen (6 mm ventral from the skull surface). A micropump (Micro4, World Precision Instruments, Sarasota, FL) delivered 0.125 U of bacterial type IV collagenase (Sigma, Oakville, ON) in 0.5 μL saline, at 250 nL/min, after which the needle was left in place for 5 min to prevent solution reflux. By avoiding the ventricles and white matter, and injecting an extremely small volume, it is very unlikely that collagenase diffused to distal areas, e.g., the contralateral hemisphere. Sham-operated animals ($n=12$) underwent the same surgical procedure, but with no collagenase in the injected saline. For all surgeries, the core temperature was maintained at 37 °C using an electric heating pad throughout surgery and recovery. Animals regained consciousness within 10 min, and no animals died as a result of the ICH or surgery.

4.2. *Minocycline treatment*

Animals with an ICH were divided into vehicle-treated ($n=32$) and minocycline-treated groups ($n=70$) and sacrificed at 1, 3 or 7 days after ICH onset. When used, minocycline was administered by intraperitoneal (i.p.) injection, with an initial dose of 45 mg/kg (at 15 mg/mL in sterile saline). The decision to use i.p. injections was based on the drug's slow release from the peritoneal cavity, which prolongs delivery (Fagan et al., 2004), reduces the frequency of injections needed, and thus reduces stress and discomfort to the rats. Animals in the 7 day survival group were further divided into two groups, with treatment for 3 or 7 days ($n=35$ each). Both groups received i.p. minocycline injections at 6 h and daily thereafter. For animals in the 7 day treatment group, the last 3 doses (at 4, 5 and 6 days) were 22.5 mg/kg. Previously, the same two-concentration dosing regime was anti-inflammatory and evoked neurobehavioral improvement (Power et al., 2003; Wasserman and Schlichter, 2007). All animals in the control, vehicle-treated group received i.p. injections of the same volume of sterile saline (0.9–1.1 mL, depending on animal weight) at the same time points as the minocycline injections.

4.3. *Quantitative real-time reverse-transcriptase polymerase chain reaction (qRT-PCR)*

4.3.1. *Tissue preparation*

ICH and sham-operated animals were sacrificed by an overdose of isofluorane at 6 h or 1, 3 or 7 days after surgery and then perfused through the heart with 100 mL phosphate buffered saline (PBS). Dissected brains were cut coronally 2 mm anterior and 2 mm posterior to the needle entry site (easily identified on the brain surface) and then divided into separate hemispheres along the midline. Each striatum was separated from surrounding white matter and cortex; hence, the tissue sample included most of the anterior caudate and putamen, and some of the globus pallidus and thalamus. In ICH animals, the sample included part of the hematoma, peri-hematoma and

Table 1 – Primers used for quantitative real-time RT-PCR

Gene	Primer name	Genbank accession #	Primer sequences
GFAP	GFAP_302	BC088851	F: CAGCTTCGAGCCAAGGAG R: TGTCCCTCTCCACCTCCA
CR3	CR3_1850	NM_012711	F: TGCTGAGACTGGAGGCAAC R: CTCCCCAGCATCCTTGTTT
IL-10	IL10_900	NM_012854	F: CCTTGGGAAGCAACTGAAAC R: GATGAGGGCAAGTGAAAGGA
IL-6	IL6_24	NM_012589	F: CAGGAACGAAAGTCAACTCCA R: ATCAGTCCCAAGAAGGCAACT
IL-1β	IL1β_487	NM_031512	F: TGACCCATGTGAGCTGAAAG R: AGGGATTTTGTCGTTGCTTG
IL-1ra/IL-1rn	IL-1ra_88	NM_022194	F: GGGAAAAGACCCTGCAAGA R: GTGGATGCCCAAGAACACA
ICE	ICE_1153	D85899	F: CCAACCACTGAAAGGGTGA R: GCATGATTCCCAACACAGG
MMP-3	MMP3_846	NM_133523	F: TCCCACAGAATCCCCTGA R: CGCCAAAAGTGCCTGTCT
MMP-9	MMP9_902	NM_031055	F: CTGCCTGCACCACTAAAGG R: GAAGACGAAGGGGAAGACG
MMP-12	MMP12_259	NM_053963	F: CTGGGCAACTGGACACCT R: CTACATCCGCACGCTTCA
TIMP-1	TIMP1_272	L31883	F: AGGTTTCCGGTTCGCCTA R: GCAGGCAGTGATGTGCAA
TACE	TACE_181	NM_020306	F: TGTGAGCAGTTTCTCGAACG R: AAAGGCACCAAAGTGGTCAG
TNFα	TNFα_277	NM_012675	F: GCCCACGTCGTAGCAAAC R: GCAGCCTTGTCCCTTGAA
TGFβ1	TGFβ1_984	NM_021578.1	F: ATACGCCTGAGTGGCTGTC R: GCCCTGTATTCCGTCTCCT
HPRT-1	HPRT1_613	XM_343829	F: CAGTACAGCCCCAAAATGGT R: CAAGGGCATATCCAACAACA

FP: forward primer; RP: reverse primer.

surrounding striatal tissue (Power et al., 2003; Wasserman and Schlichter, 2007), as shown in Fig. 9.

4.3.2. *qRT-PCR*

Gene-specific primers (Table 1) were designed with the 'Primer3-Output' program (http://frodo.wi.mit.edu/cgi-bin/primer3/primer3_www.cgi). RNeasy mini kits (Qiagen, Mississauga, ON) were used to isolate RNA after degrading any contaminating DNA with DNaseI (0.1 U/mL, 15 min, 37 °C; Amersham Biosciences, Baie d'Urfe, PQ). A two-step reaction was performed according to the manufacturer's instructions (Invitrogen, Burlington, ON); i.e., total RNA (1 μg) was reverse transcribed in 20 μL volume using 200 U of SuperScriptII RNase H-reverse transcriptase, with 0.5 mM dNTPs (Invitrogen) and 0.5 μM oligo dT (Sigma). Amplification was performed on an ABI PRISM 7700 Sequence Detection System (PE Biosystems, Foster City, CA) at 95 °C for 10 min followed by 40 cycles at 95 °C for 15 s, 56 °C for 15 s and 72 °C for 30 s. 'No-template' and 'no-amplification' controls were included for each gene. Melt curves showed a single peak, confirming specific amplification (Bustin and Nolan, 2004).

4.3.3. *Data analysis and statistics*

The threshold cycle (C_T) for each gene (Bustin and Nolan, 2004) was normalized to that of a housekeeping gene, hypoxanthine guanine phosphoribosyl transferase (HPRT1), and then results were analyzed in two stages. First, ICH-induced temporal changes in mRNA expression of all 14 genes of interest (Figs. 1–3) were assessed by comparing time-matched sham-operated animals at 6 h and 1, 3 and 7 days after ICH onset and expressed as fold changes compared with the sham-operated animals, which were normalized to 1.0. Second, minocycline-induced changes in gene expression after ICH (Fig. 4) were determined. In this case, gene expression was first normalized to time-matched sham-operated animals (which were set to 1.0) and then, treatment effects were assessed by comparing the fold change of minocycline treated animals with time-matched vehicle-treated animals. For all statistical analyses, an analysis of variance (ANOVA) was followed by Bonferroni correction, with $p<0.05$ considered significant. In all figures, the errors bars represent the standard deviation of the mean for the data presented.

4.4. *Immunohistochemistry*

At 6 h and 1, 3 and 7 days after ICH onset, 3 animals per group were sacrificed by an overdose of isofluorane and then perfused through the heart with 100 mL phosphate buffered saline (PBS) followed by 60 mL of fixative (4% paraformaldehyde, 2% sucrose in PBS; pH 7.5). Dissected brains were stored in the same fixative at 4 °C overnight followed by 10% sucrose for 24 h and 30% sucrose for 48 h. Fixed brains were cut coronally through the needle entry site, and at 4 mm anterior and 4 mm posterior to that plane. Frozen brain sections (16 μm thick) were made from the first 2 mm of tissue (the area comprising the middle of the hematoma) using a cryostat (JungCM 3000, Leica, Richmond Hill, ON) and stored at −80 °C until used. Double-labeling immunohistochemistry was performed to identify the cells that expressed IL-1β (rabbit polyclonal, 1:100; Chemicon, Temecula, CA), IL-6 (goat polyclonal 1:100; Santa Cruz, Santa Cruz, CA), IL-1ra (rabbit polyclonal, 1:100; Santa Cruz), IL-10 (goat polyclonal, 1:100; R&D, Minneapolis, MN) and MMP-12 (mouse monoclonal, 1:100; R&D). Astrocytes were visualized using an antibody against GFAP (mouse monoclonal 1:500, or rabbit polyclonal 1:500; Sigma-Aldrich, St. Louis, MO, depending on the antibody combination). Microglia/macrophages and endothelial cells were visualized using FITC-conjugated tomato lectin (1:100; Sigma-Aldrich). The secondary antibodies were Cy3-conjugated donkey anti-mouse, FITC-conjugated donkey anti-rabbit, biotin-conjugated donkey anti-goat and biotin-conjugated goat anti-rabbit. Frozen brain sections were incubated with a primary antibody for 48 h at 4 °C followed by a secondary antibody for 2 h. Sections labeled with biotin-conjugated antibodies were incubated with Cy3-conjugated streptavidin for an additional hour at room temperature. Between each step, the sections were washed three times in PBS for 5 min each. Negative controls were treated in the same manner except that the primary antibody was omitted from the staining solution.

Acknowledgments

Excellent technical help was provided by H Yang. We would like to thank V Kena-Cohen for her critical reading of the manuscript, and Drs. J Eubanks, L Mills and EF Stanley for helpful comments on the work. Supported by grants to LCS from the Heart and Stroke Foundation (HSFO; NA5158, T5546), Krembil Scientific Development Seed Fund, Canadian Stroke Network and a scholarship to JW from HSF Canada.

REFERENCES

Abilleira, S., Montaner, J., Molina, C.A., Monasterio, J., Castillo, J., Alvarez-Sabin, J., 2003. Matrix metalloproteinase-9 concentration after spontaneous intracerebral hemorrhage. J. Neurosurg. 99, 65–70.

Alvarez-Sabin, J., Delgado, P., Abilleira, S., Molina, C.A., Arenillas, J., Ribo, M., Santamarina, E., Quintana, M., Monasterio, J., Montaner, J., 2004. Temporal profile of matrix metalloproteinases and their inhibitors after spontaneous intracerebral hemorrhage: relationship to clinical and radiological outcome. Stroke 35, 1316–1322.

Barone, F.C., Feuerstein, G.Z., 1999. Inflammatory mediators and stroke: new opportunities for novel therapeutics. J. Cereb. Blood Flow Metab. 19, 819–834.

Black, R.A., Rauch, C.T., Kozlosky, C.J., Peschon, J.J., Slack, J.L., Wolfson, M.F., Castner, B.J., Stocking, K.L., Reddy, P., Srinivasan, S., Nelson, N., Boiani, N., Schooley, K.A., Gerhart, M., Davis, R., Fitzner, J.N., Johnson, R.S., Paxton, R.J., March, C.J., Cerretti, D.P., 1997. A metalloproteinase disintegrin that releases tumour-necrosis factor-alpha from cells. Nature 385, 729–733.

Brett, F.M., Mizisin, A.P., Powell, H.C., Campbell, I.L., 1995. Evolution of neuropathologic abnormalities associated with blood–brain barrier breakdown in transgenic mice expressing interleukin-6 in astrocytes. J. Neuropathol. Exp. Neurol. 54, 766–775.

Bruce, A.J., Boling, W., Kindy, M.S., Peschon, J., Kraemer, P.J., Carpenter, M.K., Holtsberg, F.W., Mattson, M.P., 1996. Altered neuronal and microglial responses to excitotoxic and ischemic brain injury in mice lacking TNF receptors. Nat. Med. 2, 788–794.

Bustin, S.A., Nolan, T., 2004. Pitfalls of quantitative real-time reverse-transcription polymerase chain reaction. J. Biomol. Tech. 15, 155–166.
Chandler, S., Cossins, J., Lury, J., Wells, G., 1996. Macrophage metalloelastase degrades matrix and myelin proteins and processes a tumour necrosis factor-alpha fusion protein. Biochem. Biophys. Res. Commun. 228, 421–429.
Clark, W.M., Rinker, L.G., Lessov, N.S., Hazel, K., Hill, J.K., Stenzel-Poore, M., Eckenstein, F., 2000. Lack of interleukin-6 expression is not protective against focal central nervous system ischemia. Stroke 31, 1715–1720.
Fagan, S.C., Edwards, D.J., Borlongan, C.V., Xu, L., Arora, A., Feuerstein, G., Hess, D.C., 2004. Optimal delivery of minocycline to the brain: implication for human studies of acute neuroprotection. Exp. Neurol. 186, 248–251.
Felberg, R.A., Grotta, J.C., Shirzadi, A.L., Strong, R., Narayana, P., Hill-Felberg, S.J., Aronowski, J., 2002. Cell death in experimental intracerebral hemorrhage: the "black hole" model of hemorrhagic damage. Ann. Neurol. 51, 517–524.
Feuerstein, G.Z., Wang, X., Barone, F.C., 1998. The role of cytokines in the neuropathology of stroke and neurotrauma. Neuroimmunomodulation 5, 143–159.
Hummel, V., Kallmann, B.A., Wagner, S., Fuller, T., Bayas, A., Tonn, J.C., Benveniste, E.N., Toyka, K.V., Rieckmann, P., 2001. Production of MMPs in human cerebral endothelial cells and their role in shedding adhesion molecules. J. Neuropathol. Exp. Neurol. 60, 320–327.
Kallmann, B.A., Wagner, S., Hummel, V., Buttmann, M., Bayas, A., Tonn, J.C., Rieckmann, P., 2002. Characteristic gene expression profile of primary human cerebral endothelial cells. FASEB J. 16, 589–591.
Lee, J.E., Yoon, Y.J., Moseley, M.E., Yenari, M.A., 2005. Reduction in levels of matrix metalloproteinases and increased expression of tissue inhibitor of metalloproteinase-2 in response to mild hypothermia therapy in experimental stroke. J. Neurosurg. 103, 289–297.
Leira, R., Davalos, A., Silva, Y., Gil-Peralta, A., Tejada, J., Garcia, M., Castillo, J., 2004. Early neurologic deterioration in intracerebral hemorrhage: predictors and associated factors. Neurology 63, 461–467.
Liberto, C.M., Albrecht, P.J., Herx, L.M., Yong, V.W., Levison, S.W., 2004. Pro-regenerative properties of cytokine-activated astrocytes. J. Neurochem. 89, 1092–1100.
Loddick, S.A., Rothwell, N.J., 1996. Neuroprotective effects of human recombinant interleukin-1 receptor antagonist in focal cerebral ischaemia in the rat. J. Cereb. Blood Flow Metab. 16, 932–940.
Loddick, S.A., Turnbull, A.V., Rothwell, N.J., 1998. Cerebral interleukin-6 is neuroprotective during permanent focal cerebral ischemia in the rat. J. Cereb. Blood Flow Metab. 18, 176–179.
Lu, A., Tang, Y., Ran, R., Ardizzone, T.L., Wagner, K.R., Sharp, F.R., 2006. Brain genomics of intracerebral hemorrhage. J. Cereb. Blood Flow Metab. 26, 230–252.
Lucas, S.M., Rothwell, N.J., Gibson, R.M., 2006. The role of inflammation in CNS injury and disease. Br. J. Pharmacol. 147 (Suppl 1), S232–S240.
Maier, C.M., Hsieh, L., Crandall, T., Narasimhan, P., Chan, P.H., 2006. Evaluating therapeutic targets for reperfusion-related brain hemorrhage. Ann. Neurol. 59, 929–938.
Masada, T., Hua, Y., Xi, G., Yang, G.Y., Hoff, J.T., Keep, R.F., 2001. Attenuation of intracerebral hemorrhage and thrombin-induced brain edema by overexpression of interleukin-1 receptor antagonist. J. Neurosurg. 95, 680–686.
Moss, M.L., et al., 1997. Cloning of a disintegrin metalloproteinase that processes precursor tumour-necrosis factor-alpha. Nature 385, 733–736.
Mulcahy, N.J., Ross, J., Rothwell, N.J., Loddick, S.A., 2003. Delayed administration of interleukin-1 receptor antagonist protects against transient cerebral ischaemia in the rat. Br. J. Pharmacol. 140, 471–476.
Pekny, M., Nilsson, M., 2005. Astrocyte activation and reactive gliosis. Glia 50, 427–434.
Penkowa, M., Giralt, M., Lago, N., Camats, J., Carrasco, J., Hernandez, J., Molinero, A., Campbell, I.L., Hidalgo, J., 2003. Astrocyte-targeted expression of IL-6 protects the CNS against a focal brain injury. Exp. Neurol. 181, 130–148.
Power, C., Henry, S., Del Bigio, M.R., Larsen, P.H., Corbett, D., Imai, Y., Yong, V.W., Peeling, J., 2003. Intracerebral hemorrhage induces macrophage activation and matrix metalloproteinases. Ann. Neurol. 53, 731–742.
Qureshi, A.I., Suri, M.F., Ostrow, P.T., Kim, S.H., Ali, Z., Shatla, A.A., Guterman, L.R., Hopkins, L.N., 2003. Apoptosis as a form of cell death in intracerebral hemorrhage. Neurosurgery 52, 1041–1047.
Rosell, A., Ortega-Aznar, A., Alvarez-Sabin, J., Fernandez-Cadenas, I., Ribo, M., Molina, C.A., Lo, E.H., Montaner, J., 2006. Increased brain expression of matrix metalloproteinase-9 after ischemic and hemorrhagic human stroke. Stroke 37, 1399–1406.
Rosenberg, G.A., 2002. Matrix metalloproteinases in neuroinflammation. Glia 39, 279–291.
Rosenberg, G.A., Mun-Bryce, S., Wesley, M., Kornfeld, M., 1990. Collagenase-induced intracerebral hemorrhage in rats. Stroke 21, 801–807.
Silva, Y., Leira, R., Tejada, J., Lainez, J.M., Castillo, J., Davalos, A., 2005. Molecular signatures of vascular injury are associated with early growth of intracerebral hemorrhage. Stroke 36, 86–91.
Singhal, A., Baker, A.J., Hare, G.M., Reinders, F.X., Schlichter, L.C., Moulton, R.J., 2002. Association between cerebrospinal fluid interleukin-6 concentrations and outcome after severe human traumatic brain injury. J. Neurotrauma 19, 929–937.
Stirling, D.P., Koochesfahani, K.M., Steeves, J.D., Tetzlaff, W., 2005. Minocycline as a neuroprotective agent. Neuroscientist 11, 308–322.
Streit, W.J., Walter, S.A., Pennell, N.A., 1999. Reactive microgliosis. Prog. Neurobiol. 57, 563–581.
Stroemer, R.P., Rothwell, N.J., 1998. Exacerbation of ischemic brain damage by localized striatal injection of interleukin-1beta in the rat. J. Cereb. Blood Flow Metab. 18, 833–839.
Szymanska, A., Biernaskie, J., Laidley, D., Granter-Button, S., Corbett, D., 2006. Minocycline and intracerebral hemorrhage: influence of injury severity and delay to treatment. Exp. Neurol. 197, 189–196.
Tang, Y., Lu, A., Aronow, B.J., Wagner, K.R., Sharp, F.R., 2002. Genomic responses of the brain to ischemic stroke, intracerebral haemorrhage, kainate seizures, hypoglycemia, and hypoxia. Eur. J. Neurosci. 15, 1937–1952.
Tejima, E., Zhao, B.Q., Tsuji, K., Rosell, A., van, L.K., Gonzalez, R.G., Montaner, J., Wang, X., Lo, E.H., 2007. Astrocytic induction of matrix metalloproteinase-9 and edema in brain hemorrhage. J. Cereb. Blood Flow Metab. 27, 460–468.
Tsuji, M., Wilson, M.A., Lange, M.S., Johnston, M.V., 2004. Minocycline worsens hypoxic–ischemic brain injury in a neonatal mouse model. Exp. Neurol. 189, 58–65.
Vila, N., Castillo, J., Davalos, A., Chamorro, A., 2000. Proinflammatory cytokines and early neurological worsening in ischemic stroke. Stroke 31, 2325–2329.
Wang, J., Dore, S., 2007. Inflammation after intracerebral hemorrhage. J. Cereb. Blood Flow Metab. 27, 894–908.
Wang, J., Tsirka, S.E., 2005. Neuroprotection by inhibition of matrix metalloproteinases in a mouse model of intracerebral haemorrhage. Brain 128, 1622–1633.
Wasserman J.K., Schlichter L.C., in press. Minocycline protects the blood–brain barrier and reduces edema following intracerebral hemorrhage in the rat. Exp. Neurol. doi:10.1016/j.expneurol.2007.06.025.
Wasserman, J.K., Schlichter, L.C., 2007. Neuron death and

inflammation in a rat model of intracerebral hemorrhage: effects of delayed minocycline treatment. Brain Res. 1136, 208–218.
Wells, J.E., Biernaskie, J., Szymanska, A., Larsen, P.H., Yong, V.W., Corbett, D., 2005. Matrix metalloproteinase (MMP)-12 expression has a negative impact on sensorimotor function following intracerebral haemorrhage in mice. Eur. J. Neurosci. 21, 187–196.
Wilson, K.P., Black, J.A., Thomson, J.A., Kim, E.E., Griffith, J.P., Navia, M.A., Murcko, M.A., Chambers, S.P., Aldape, R.A., Raybuck, S.A., 1994. Structure and mechanism of interleukin-1 beta converting enzyme. Nature 370, 270–275.
Xue, M., Del Bigio, M.R., 2000. Intracerebral injection of autologous whole blood in rats: time course of inflammation and cell death. Neurosci. Lett. 283, 230–232.
Yang, G.Y., Zhao, Y.J., Davidson, B.L., Betz, A.L., 1997. Overexpression of interleukin-1 receptor antagonist in the mouse brain reduces ischemic brain injury. Brain Res. 751, 181–188.
Yenari, M.A., Xu, L., Tang, X.N., Qiao, Y., Giffard, R.G., 2006. Microglia potentiate damage to blood–brain barrier constituents: improvement by minocycline in vivo and in vitro. Stroke 37, 1087–1093.
Yong, V.W., Power, C., Forsyth, P., Edwards, D.R., 2001. Metalloproteinases in biology and pathology of the nervous system. Nat. Rev., Neurosci. 2, 502–511.
Yrjanheikki, J., Keinanen, R., Pellikka, M., Hokfelt, T., Koistinaho, J., 1998. Tetracyclines inhibit microglial activation and are neuroprotective in global brain ischemia. Proc. Natl. Acad. Sci. U. S. A. 95, 15769–15774.
Yrjanheikki, J., Tikka, T., Keinanen, R., Goldsteins, G., Chan, P.H., Koistinaho, J., 1999. A tetracycline derivative, minocycline, reduces inflammation and protects against focal cerebral ischemia with a wide therapeutic window. Proc. Natl. Acad. Sci. U. S. A. 96, 13496–13500.
Zhao, B.Q., Wang, S., Kim, H.Y., Storrie, H., Rosen, B.R., Mooney, D.J., Wang, X., Lo, E.H., 2006. Role of matrix metalloproteinases in delayed cortical responses after stroke. Nat. Med. 12, 441–445.